Hysteresis-like effects in gyrotron oscillators

Hysteresis-like effects in gyrotron oscillators

O. Dumbrajs, T. Idehara, Y. Iwata, and S. Mitsudo
Research Center for Development of Far-Infrared Region, Fukui University, Bunkyo 3-9-1, Fukui 910-8507, Japan

I. Ogawa
Cryogenic Laboratory, Faculty of Engineering, Fukui University, Bunkyo 3-9-1, Fukui 910-8507, Japan

B. Piosczyk
Forschungszentrum Karlsruhe, Institut für Hochleistungsimpuls- und Mikrowellentechnik, Association Euratom FZK, Hermann von-Helmholtz-Platz 1, D-76344 Eggenstein-Leopoldshafen, Germany

Special experiments devoted to studying hysteresis in gyrotron oscillators have been performed for the first time. Clear hysteresis-like effects with respect to variation of the cathode voltage have been observed in the mode competition scenario of the Forschungszentrum Karlsruhe coaxial gyrotron [B. Piosczyk *et al.*, IEEE Trans. Plasma Sci. **30**, 818 (2002)] and with respect to variation of the magnetic field and voltage in a single-mode operation of the Fukui IV gyrotron [T. Idehara *et al.*, Int. J. Infrared Millim. Waves **19**, 793 (1998)]. The observed phenomena are explained theoretically.

Gyrotrons are microwave sources whose operation is based on the stimulated cyclotron radiation of electrons oscillating in a static magnetic field. Gyrotron devices are now able to generate several orders of magnitude as much power at millimeter wavelength as classical microwave tubes, and can operate at frequencies higher than are conveniently available from other types of tubes. Gyrotron oscillators can have a wide application, including radars, advanced communication systems, technological processes, atmospheric sensing, ozone conservation, artificial ionospheric mirror, extra-high-resolution spectroscopy, etc. However, the main application of powerful gyrotrons is electron cyclotron resonance plasma heating in tokamaks and stellarators and the noninductive current drive in tokamaks. Extensive literature exists on various aspects of these microwave tubes.[1] The study of one very interesting phenomenon—hysteresis—has been neglected so far, although perfect understanding of hysteresis is important in connection with mode competition, frequency tuning, voltage overshooting, amplitude modulation of the signal, etc. In gyrotrons hysteresis is the phenomenon that causes the amplitude of oscillations to lag behind the magnetic field and the voltage, so that operation regions of modes for rising and falling magnetic field and voltage are not the same.

In nonlinear oscillator theory[2] hysteresis is intimately linked to existence of the so-called hard excitation region, where for certain parameter values of the system, stable oscillations can be induced only by kicking the oscillator with the amplitude that is larger than the stationary one. Since, like most of the oscillators, a gyrotron is a very nonlinear system, it was no surprise that hard excitation regions were discovered at the advent of gyrotron research.[3–5] During the past decades existence of hard excitation region in gyrotrons has been mentioned on many occasions (see, e.g., Refs. 6 and 7), albeit without mentioning explicitly hysteresis.

In this Letter, we present the first devoted experimental verification of different hysteresis-like phenomena in gyrotrons predicted by a theory as well as describe this theory.

The Forschungszentrum Karlsruhe (FZK) coaxial gyrotron[8] operates in pulsed regime. Measurements of hysteresis have been performed for the constant magnetic field $B = 6.66$ T. The oscillating range for single mode operation of the nominal $TE_{31,17}$ (165 GHz) mode has been measured for different beam currents for rising and falling cathode voltage U_c. The results are shown in Fig. 1(a).

For rising voltage first the $TE_{32,17}$ mode oscillates. On the high voltage side either the $TE_{30,17}$ mode or at larger beam currents the $TE_{29,17}$ mode are oscillating. In between the nominal $TE_{31,17}$ mode is oscillating. The boundaries of its oscillating range are shown in the figure. Figure 1(b) gives the rf power calculated for a beam current $I_b = 50$ A at

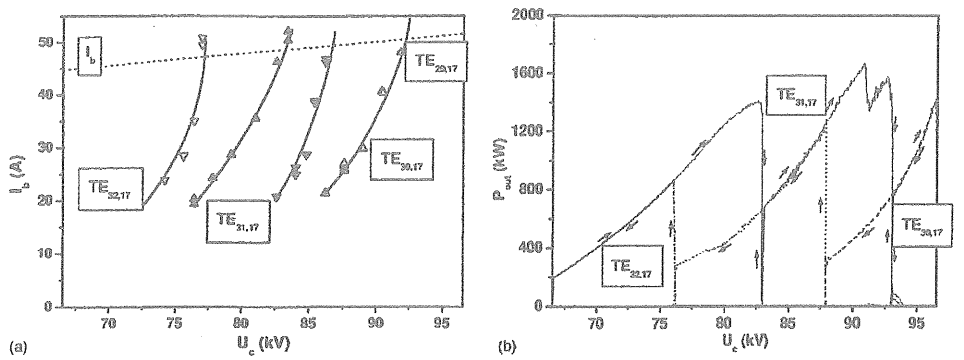

FIG. 1. Hysteresis in the FZK coaxial gyrotron with respect to variation of the cathode voltage. (a) Experimental oscillating range of the nominal mode $TE_{31,17}$ starts at (▲) and ends at (△), whereas for decreasing voltage the $TE_{31,17}$ mode oscillates in the range between (▼) and (▽). The dotted curve shows the beam current dependence on U_c. (b) Radio frequency power calculated for the beam current $I_b = 50$ A at $U_c = 90$ kV. The arrows correspond to the rising (→) and falling (←) cathode voltage.

$U_c = 90$ kV. In good agreement with the experiment the calculations reproduce the hysteresis behavior. Depending on the direction of the voltage variation, indicated in the figure by the arrows, the oscillating range of the modes is changing due to the hysteresis effect. In conformity with theoretical predictions (Fig. 5) the hysteresis increases with increasing beam current exceeding 5 kV for $I_b = 50$ A.

Three important conclusions can be drawn from the results presented in Fig. 1. First, the hysteresis influences mode competition and it should be taken into account in designing frequency-step-tunable gyrotrons for plasma physics applications[9] based on voltage variation as proposed in Ref. 10. The use of the present gyrotron as a frequency-step-tunable source at frequencies 167.27 GHz ($TE_{32,17}$), 165.00 GHz ($TE_{31,17}$), and 162.72 GHz ($TE_{30,17}$) in the case of rising voltage would require the sequence of U_c: 82 kV→92 kV→95 kV. For the falling voltage the hysteresis loops have to be included and U_c should be changed as 95 kV→87.5 kV→92 kV to obtain oscillations in the $TE_{31,17}$ mode, and 92 kV→76 kV→82 kV to obtain oscillations in the $TE_{32,17}$ mode. Second, due to hysteresis the voltage overshooting during ramp-up becomes dangerous. To obtain maximum output power in the nominal $TE_{31,17}$ mode at $U_c = 92$ kV, one has to avoid voltage overshooting larger than ~1 kV. Otherwise the gyrotron at lower voltages will oscillate in the wrong $TE_{30,17}$ mode, delivering a significantly lower power. Third, hysteresis makes it possible to decrease the lower bound of the region of amplitude modulation from ~83 kV(600 kW) to ~76 kV(250 kW).

The low-power and low-mode gyrotrons[11–14] are especially suitable for studying hysteresis phenomena, because they allow investigation of additional effects that is not possible in high-power high-mode gyrotrons.

Such gyrotrons can oscillate in well-separated low-order modes that allow studying hysteresis without taking into account mode competition. They can operate in the CW regime and hence permit studying hysteresis with respect to variation of the magnetic field. A clear experimental hysteresis loop with respect to such a variation was observed in the Sydney gyrotron and reported in Ref. 11, albeit without relating it to any theory. In Fig. 2 we show such a hysteresis in the Fukui IV gyrotron in the operation region of the $TE_{0,3}$ mode oscillating at 302.20 GHz at the fixed anode and cathode voltages. The hysteresis loop is ~0.003 T.

In Fig. 3 we show hysteresis with respect to variation of the cathode voltage at the fixed magnetic field and anode voltage. The hysteresis loop is ~0.35 kV.

In Fig. 4 we show hysteresis with respect to variation of the anode voltage U_a at the fixed magnetic field and cathode voltage. The measured loop is very narrow, ~0.02 kV, which

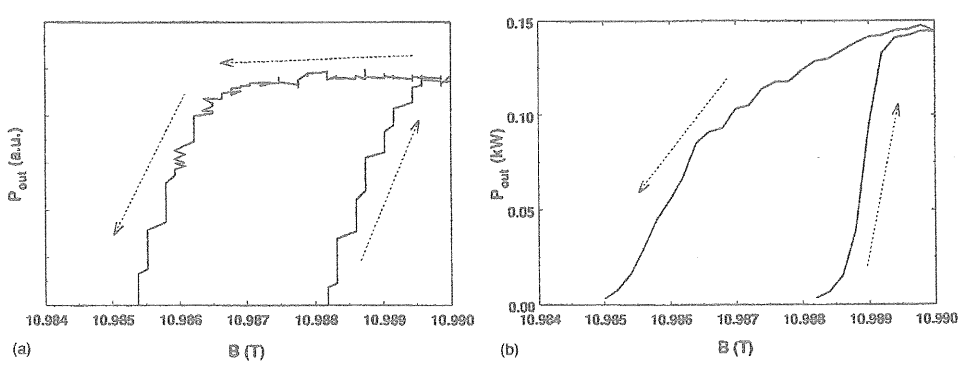

FIG. 2. Hysteresis in the Fukui IV gyrotron with respect to variation of the magnetic field. (a) Experimental oscillating range of the $TE_{0,3}$ mode. (b) Radio frequency power calculated for the beam current $I_b = 0.07$ A, $U_a = 6.8$ kV, and $U_c = 14.2$ kV.

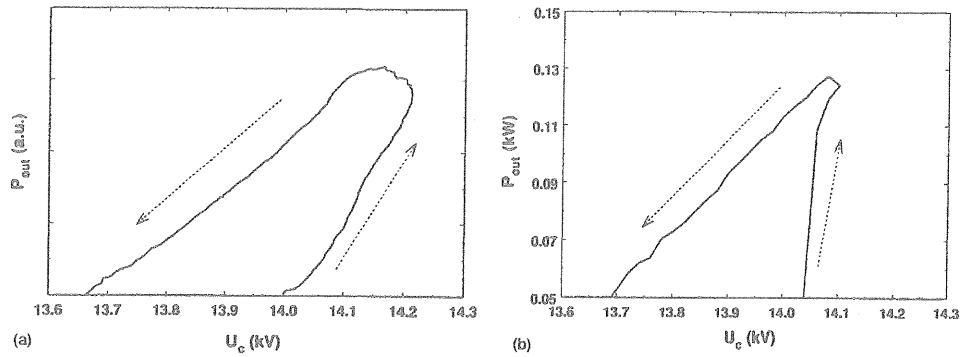

FIG. 3. Hysteresis in the Fukui IV gyrotron with respect to variation of the cathode voltage. (a) Experimental oscillating range of the $TE_{0,3}$ mode. (b) frequency power calculated for the beam current $I_b=0.07$ A, $U_a=6.8$ kV, and $B=10.99$ T.

is related to the fact that in this case, in contrast to variable B and U_c, we are moving almost "parallel" to the curves shown in Fig. 5.

Theoretically hysteresis can be studied most conveniently using a time-dependent equation for the oscillation amplitude. In such calculations the equation is solved for a given fixed value of the parameter of interest (B, U_a, or U_c) until the onset of stationary oscillations. After this the parameter is increased by a small amount and calculations are continued until again the onset of stationary oscillations. This is repeated until the desired parameter value is reached. Next such calculations are carried out in the reverse direction with decreasing parameter values. Theoretical computations presented in this article are based on the following system of partial differential equations[15] which describe self-consistently multimode gyrotron oscillations:

$$\begin{aligned}&(\partial p/\partial\zeta)+i(|p|^2-1)p=i\sum_s f_s\exp[i(\Delta_s\zeta+\psi_s)],\\&(\partial^2 f_s/\partial\zeta^2)-i(\partial f_s/\partial\tau)+\delta_s f_s\\&\quad=I_s(1/4\pi^2)\int_0^{2\pi}\int_0^{2\pi}p\,\vartheta_0\exp[-i(\Delta_s\zeta+\psi_s)]\,d\phi.\end{aligned}\tag{1}$$

Here p is the complex transverse momentum of the electron normalized to its initial absolute value, $\zeta=(\beta_\perp^2\omega_c/2\beta_\parallel c)z$ is the dimensionless longitudinal coordinate, $\beta_\parallel=v_\parallel/c$ and $\beta_\perp=v_\perp/c$ are normalized electron velocities, c is the velocity of light, z is the longitudinal coordinate, $f_s(\zeta,\tau)$ is the rf field in the resonator, $\Delta_s=2\beta_\perp^{-2}(\omega_s-\omega_c)\omega_s^{-1}$ is the frequency mismatch, ω_s is the rf frequency, $\omega_c[\mathrm{GHz}]=56\pi B[\mathrm{T}]/\gamma_{\mathrm{rel}}$ is the electron cyclotron frequency, B is the magnetic field in the resonator, $\gamma_{\mathrm{rel}}=1+U_c[\mathrm{kV}]/511$ is the relativistic factor, $\psi_s=8\beta_\parallel^2\beta_\perp^{-4}(\overline{\omega_s}-\omega_c)\omega_c^{-1}\tau+(1\mp m_s)\phi$ is the phase of the mode, m_s and ϕ are the azimuthal index and coordinate, respectively, $\tau=\frac{1}{8}\beta_\perp^4\beta_\parallel^{-2}\omega_c t$ is the dimensionless time, t is time, $\delta_s=8\beta_\parallel^2\beta_\perp^{-4}[\overline{\omega_s}-\omega_{s,\mathrm{cut}}(\zeta)]\omega_c^{-1}$ describes variation of the cut-off frequency $\omega_{s,\mathrm{cut}}(\zeta)$ along the resonator axis, $\overline{\omega_s}$ is the cut-off frequency at the exit from the resonator, and I_s is the dimensionless current which includes the rf field and electron beam coupling:

$$I_s=9.4\times10^{-4}I_b[A]\beta_\parallel\beta_\perp^{-6}\frac{J_{m_s\pm1}^2((2\pi/\lambda_s)R_{el})}{\gamma_{rel}(\nu_s^2-m_s^2)J_{m_s}^2(\nu_s)},\tag{2}$$

where λ_s is the wavelength, R_{el} is the electron beam radius, and ν_s is the eigenvalue. The subscript s refers to the sth mode.

The first equation in the system (1) has to be supplemented by the initial condition $p(0)=\exp(\vartheta_0)$ with $0\leq\vartheta_0<2\pi$ and the second equation by the boundary condition at the end of the exit cone of the resonator:

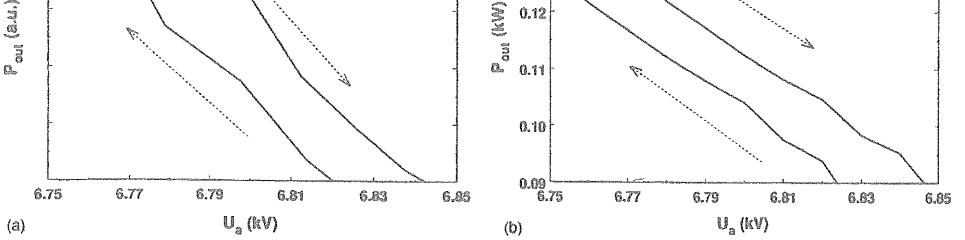

FIG. 4. Hysteresis in the Fukui IV gyrotron with respect to variation of the anode voltage. (a) Experimental oscillating range of the $TE_{0,3}$ mode. (b) Radio frequency power calculated for the beam current $I_b=0.07$ A, $U_c=14.0$ kV, and $B=10.99$ T.

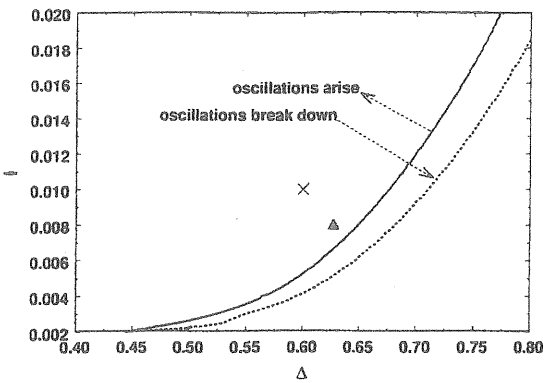

FIG. 5. Oscillation regions in the $\Delta - I$ plane. The upper curve is the border of arising and the lower curve the border of breakdown of oscillations. Without hysteresis these two borders would coincide. The point of the maximum efficiency ($\eta_\perp = 0.75$) is marked by × and the approximate operation point of the Fukui FU IV gyrotron is marked by ▲.

$$[\partial f_s(\zeta,\tau)/\partial\zeta + ik_s f_s(\zeta,\tau)]\big|_{\zeta=\zeta_{\text{out}}} = 0, \tag{3}$$

where $k_s = 2c\beta_\parallel\beta_\perp^{-2}\omega_c^{-1}\sqrt{\omega_s^2/c^2 - \nu^2(\zeta)/R_{\text{cav}}^2(\zeta)}$ is the dimensionless wave number and R_{cav} is the cavity radius.

The curves shown in Fig. 1(b) were obtained by solving numerically Eq. (1) with inclusion of seven competing modes. The theoretical results presented in Figs. 2(b), 3(b), and 4(b) were obtained in a single-mode approximation. Here the method developed in Ref. 16 was used in the numerical integration. It is based on the fully implicit scheme of solving parabolic differential equations.

The hysteresis in gyrotrons for a single mode can be theoretically illustrated in the most general manner by plotting oscillation regions in the $\Delta - I$ plane.

The curves shown in Fig. 5 correspond to the case $\zeta_{\text{out}} = 15$ which represents a typical length of gyrotron resonators. In gyrotrons two types of electron guns are used. In the case of a diode gun (FZK gyrotron) there is no anode voltage and the electron velocities depend only on U_c. In a triode gun (Fukui gyrotrons) they depend also on the anode voltage U_a and on some geometrical parameters of the gun (see, e.g., Refs. 1 and 7 for such dependences). The functions $\beta_\perp(B,U_a,U_c)$ and $\beta_\parallel(B,U_a,U_c)$ have to be known very accurately for a specific gun, in order to make quantitative predictions of hysteresis loops in a specific gyrotron. It is well known that in practice it is not always easy to obtain such information reliably. For this reason the comparison between experiment and theory presented in Figs. 2–4 should be regarded as qualitative.

We would like to mention another, albeit exotic, possible hysteresis-like phenomenon in gyrotrons: hysteresis with respect to variation of the cavity length. Such a phenomenon can be envisaged by examining gyrotron efficiency plots in the $I - \mu$ plane (see, e.g., Fig. 5 in Ref. 6). Since the dimensionless cavity length $\mu = \pi(\beta_\perp^2/\beta_\parallel)(L/\lambda)$ is proportional to the real cavity length L, by varying only the latter we are moving between the soft and hard excitation regions, which, as stated above, is linked to hysteresis. It can hardly be expected that such an experiment will be carried out in practice. However, indirectly this idea gets support from the results discussed in Ref. 17 where simulations of a gyroklystron have revealed hysteresis-like features in the drive curve. This was attributed to the variable interaction space in the output cavity.

In summary, we have presented a compact report on hysteresis-like effects in gyrotron oscillators. The two devoted experimental measurements of various hysteresis loops demonstrate to our opinion an excellent qualitative agreement between theory and experiment. The results of the work impose quantitative limits on the expected magnitude of hysteresis. New more accurate experiments are needed to quantify our understanding of this very interesting phenomenon.

[1] *Gyrotron Oscillators: Their Principles and Practice*, edited by C. J. Edgcombe (Taylor & Francis, London, 1993).

[2] N. N. Bogolyubov and Y. A. Mitropolsky, *Asymptotic Methods in the Theory of Nonlinear Oscillations* (Hindustan, India, 1961), pp. 91–104.

[3] M. A. Moiseev, G. G. Rogacheva, and V. K. Yulpatov, "Theoretical studies of influence of the longitudinal inhomogeneity of the electromagnetic field in a resonator on the efficiency of a CRM-monotron," *Proceedings of the All-Union Conference Devoted to Radio Day, Moscow, 1968* (Popov, Moscow, 1968), p. 68 (in Russian).

[4] G. S. Nusinovich and R. E. Erm, Electron. Tech., Ser. 1, Electron. SVCh **8**, 55 (1972).

[5] D. V. Kisel, G. S. Korablev, V. G. Pavelyev, M. I. Petelin, and Sh. E. Tsimring, Radio Eng. Electron. Phys. **19**, 95 (1974).

[6] B. Danly and R. Temkin, Phys. Fluids **29**, 561 (1986).

[7] D. R. Whaley, M. Q. Tran, T. M. Tran, and T. M. Antonsen, IEEE Trans. Plasma Sci. **22**, 850 (1994).

[8] B. Piosczyk, A. Arnold, G. Dammertz, O. Dumbrajs, M. Kuntze, and M. Thumm, IEEE Trans. Plasma Sci. **30**, 819 (2002).

[9] O. Dumbrajs, J. A. Heikkinen, and H. Zohm, Nucl. Fusion **41**, 927 (2001).

[10] O. Dumbrajs and G. S. Nusinovich, IEEE Trans. Plasma Sci. **20**, 452 (1992).

[11] G. F. Brand, T. Idehara, T. Tatsukawa, and I. Ogawa, Int. J. Electron. **72**, 745 (1992).

[12] T. Idehara, K. Yoshida, N. Nishida, I. Ogawa, M. L. Pereyaslavets, and T. Tatsukawa, Infared Millim. Waves **19**, 793 (1998).

[13] I. Ogawa, T. Idehara, Y. Iwata, R. Pavlichenko, S. Mitsudo, D. Wagner, and M. Thumm, in Proceedings of the 27th International Conference on Infrared and Millimeter Waves, San Diego, CA, 22–26 September 2002, edited by J. Temkin, pp. 293–294.

[14] T. Idehara, K. Ichikawa, I. Ogawa, T. Tatsukawa, and G. F. Brand, Int. J. Infrared Millim. Waves **19**, 1607 (1998).

[15] N. A. Zavolsky, G. S. Nusinovich, and A. B. Pavelyev, in *Gyrotrons* (Academy of Sciences of USSR, Gorky, 1989), p. 84 (in Russian).

[16] M. I. Airila, O. Dumbrajs, A. Reinfelds, and U. Strautiņš, Phys. Plasmas **8**, 4608 (2001).

[17] A. Salop and M. Caplan, Int. J. Electron. **61**, 1005 (1986).